Correlated time derivatives of current, electric field intensity, and magnetic flux density for triggered lightning at 15 m

M. A. Uman, J. Schoene, V. A. Rakov, K. J. Rambo, and G. H. Schnetzer
Department of Electrical and Computer Engineering, University of Florida, Gainesville, Florida, USA

Received 11 December 2000; revised 25 July 2001; accepted 18 October 2001; published 2 July 2002.

[1] We present measured current and its time derivative correlated with the corresponding electric field intensity and magnetic flux density and their time derivatives measured at 15 m for two lightning return strokes triggered in 1999 at Camp Blanding, Florida. Lightning was triggered to a vertical 2-m rod mounted at the center of a 70 × 70 m buried metallic grid. The rocket-launching system was located underground at the center of the grid. The experiment was designed to minimize any influence of either the strike object or a finite-conducting Earth (ground surface arcing and propagation effects) on the fields and field derivatives. The measured current derivative waveform and the return stroke portion of the magnetic flux density derivative and electric field intensity derivative waveforms associated with the two strokes are observed to be essentially unipolar pulses that have similar waveshapes for the first 150 ns or so, including the initial rising portion, the peak, and about 50 ns after the peak. The current and magnetic field derivative waveshapes are very similar for their total duration, and both decay to near zero about 200 ns after the peak derivative is reached. The electric field derivative decays more slowly than the current derivative after about 150 ns, taking about 500 ns to decay to near zero. The transmission-line model, the simplest available and most used return stroke model, is employed to calculate the return stroke field derivatives, given the measured current derivative as a model input, for return stroke speeds of 1×10^8 m s^{-1}, 2×10^8 m s^{-1}, and 3×10^8 m s^{-1} (the speed of light). A reasonable match between calculated and measured field derivative waveshapes is achieved for both strokes for a return stroke speed between 2×10^8 m s^{-1} and 3×10^8 m s^{-1}. Although the measured field and current derivatives have similar waveshapes for about 150 ns, which might appear to be consistent with the hypothesis that the radiation field component of the total field derivative is dominant for that time, transmission line model calculations indicate that this is not the case. Further, electric field derivatives measured simultaneously at 15 m and at 30 m for many strokes are observed to have similar waveshapes, which also might appear to be consistent with the hypothesis that the derivatives are dominated by the radiation field component; however, according to transmission line model calculations, while the calculated total field derivative waveshapes are similar at 15 and 30 m, all field components significantly contribute to the waveforms at both distances, and the mix of field components at 15 m and at 30 m is quite different. *INDEX TERMS:* 3324 Meteorology and Atmospheric Dynamics: Lightning; 3304 Meteorology and Atmospheric Dynamics: Atmospheric electricity; 3367 Meteorology and Atmospheric Dynamics: Theoretical modeling; *KEYWORDS:* Lightning, atmospheric electricity

1. Introduction

[2] *Uman et al.* [2000] have reviewed the literature on the measured time derivative of the electric field intensity for both natural and triggered lightning return strokes, and they have presented their own electric field derivative data at 10 to 30 m from triggered lightning return strokes. They argue, using both their own data and those in the literature, that the electric field derivative from triggered lightning and, by inference, from natural lightning subsequent return strokes, can be significantly influenced by the height of the structure on which the lightning terminates. Further, they report that their electric field derivative and current derivative waveforms are similar well past the peaks of the derivative pulses, although this conclusion is not completely convincing since they employed noisy and bandwidth-limited current derivative data. *Uman et al.* [2000] discuss the implications of the similarity in current and electric field derivative waveforms at early times as regards to the relative contribution of the individual components (electrostatic, induction, and radiation) to the total electric field derivative. This waveshape similarity and the similarity of their electric field derivative waveshapes at 10 m and at

0148-0227/02/2000JD000249$09.00

30 m is consistent with the hypothesis of a dominant radiation field, a hypothesis which is at odds with theoretical arguments based on antenna theory presented by *Uman et al.* [2000] and calculations based on the transmission line model by *Cooray* [1989] and by *Leteinturier et al.* [1990]. *Uman et al.* [2000] conclude that simultaneous measurements of both electric and magnetic field derivatives, along with the current derivative, could well help clarify the issue.

[3] In the present paper we report on a rocket-triggered lightning experiment in which the derivatives of the electric field intensity and magnetic flux density at 15 and 30 m and the causative current derivative were measured simultaneously for two strokes. Also measured were the current, electric field intensity, and magnetic flux density. The experimental setup was designed to minimize any potential influence on the fields and field derivatives of the strike object, ground surface arcing [*Rakov et al.*, 1998], or the effects of propagation over a finitely conducting Earth. The transmission line model [*Uman and McLain*, 1969] is used in an attempt to gain insight into the relationship between the measured field and current derivative waveforms as well as the influence of the value of the return stroke speed for the two return strokes for which a complete data set was recorded. The model is also used to examine the observed absence of distance dependence of the electric field derivative waveshapes.

2. Experiment

[4] Lightning was artificially initiated (triggered) from natural thunderclouds using the rocket-and-wire technique [e.g., *Rakov et al.*, 1998] at the International Center for Lightning Research and Testing at Camp Blanding, Florida, during the summer of 1999. A photograph of the experimental site looking east during triggered lightning flash S9934 is found in Figure 1. Additionally, using video records of flash S9934 taken looking east and south, we determined that during the flash the overall channel of S9934 moved in a westerly direction a few meters with the prevailing wind and, in the bottom 5 m or so, was initially vertical and then leaned toward the west. For the later strokes S9934-6 and S9934-7, modeled here, the bottom 5 m or so leaned west at an angle of about 40°, and above the bottom 5 m or so, the channel was more or less straight and leaned toward the east about 20° from the vertical, that is, into the page in Figure 1. The rocket launcher was located underground with the strike object being a metal rod extending from the rocket launcher to 2 m above ground level, as seen in Figure 1. The launcher and rod were in the center of a 70 × 70 m metal mesh grid, intended to simulate a perfectly conducting ground plane, which was covered by some centimeters of dirt. The metal mesh grid exhibited a low-frequency, low-current ground resistance of about 6 Ω. A 16.5-m-long ground rod was installed beneath the rocket launcher and was bonded to the plane and to the rocket launcher. The ground rod exhibited a low-frequency, low-current ground resistance of about 40 Ω. The derivative of the current in the strike rod was measured with an EG&G IMM-5 I-Dot sensor mounted at the base of the strike rod. The current derivative signal was transmitted by Nanofast fiber optic links to the measurement facility 50 m away where the signal was low-pass filtered

Figure 1. A photograph of the experimental site and triggered lightning flash S9934. A magnetic field antenna is seen on the right.

with a 3-dB bandwidth of 20 MHz and then digitized at 250 MHz. The current into the metal mesh grid and into the ground rod were digitized separately at 50 MHz after being low-pass filtered with a 3-dB bandwidth of 20 MHz. The total current is obtained as the sum of the two separately measured current components. The electric field antenna and the electric field derivative antenna were flat plate antennas that sensed the vertical components of the field and field derivative, as described by *Uman et al.* [2000] and *Crawford et al.* [2001]. The magnetic field and magnetic field derivative antennas were shielded wire loops measuring the azimuthal component of the field in a horizontal plane relative to the strike point. One loop antenna is seen in Figure 1. The 3-dB bandwidth of the electric and magnetic field derivative measurements was 20 MHz including the Meret fiber optic links, of the electric field intensity measurement was 10 MHz at 15 m and 20 MHz at 30m, and of the magnetic flux density measurements was 4 MHz, all bandwidths being determined by the use of low-pass filters prior to signal digitization. The electric and magnetic fields were digitized at 25 MHz, and their derivatives were digitized at 250 MHz, except for the magnetic field derivative at 30 m which was digitized at 50 MHz. The electric field and electric field derivative antennas were calibrated using theory for amplitude and laboratory tests for waveform fidelity [*Uman et al.*, 2000], as were the magnetic field and magnetic field derivative antennas. From a comparison of the outputs of different antennas at different locations on the ground plane but at the same distance from the same lightning event, we estimate the potential amplitude calibration errors to be about 20%. We used the manufacturer's calibration for the current and current derivative sensors. All fiber optic links were calibrated independently.

[5] For only 2 strokes out of 54 total recorded strokes in 11 flashes triggered from the underground launcher in 1999 did we obtain a complete data set: electric and magnetic fields and field derivatives at 15 m, current, and current derivative. For all other strokes some of the data were either saturated or are unavailable because of system failures. Often, lightning did not attach to the strike rod so that the current derivative could not be directly recorded. We obtained simultaneous fields and field derivatives at 15 and 30 m for many strokes, but none for which the current derivative was simultaneously measured. Here we primarily examine the two strokes from flash S9934 for which we obtained a complete data set for fields and field derivatives

at 15 m. The peak current derivatives for these two strokes, 80 and 100 kA μs^{-1}, are at the lower end of the observed current derivative amplitude distribution, which ranged from 80 to 290 kA μs^{-1}. The peak currents, 8.5 and 11 kA, are also at the lower end of the observed range of currents, 8.1 to 35 kA.

3. Data

[6] In Figures 2a and 2b we present a complete set of measurements (current I, current derivative dI/dt, electric field intensity E, electric field intensity derivative dE/dt, magnetic flux density B, and magnetic flux density derivative dB/dt), the latter four measurements being taken at 15 m for strokes S9934-6 and S9934-7. These strokes were the sixth and seventh in flash S9934. Both strokes lowered negative charge to ground, and the current is arbitrarily plotted as negative. The atmospheric electricity sign convention (downward directed electric field vector is defined as positive) is used in plotting E and dE/dt. In Figures 3a and 3b and Figures 4a and 4b the current derivative, magnetic flux density derivative, and electric field intensity derivative are overlaid for strokes S9934-6 and S9934-7 on two timescales, showing the similarity in waveshapes of these signals for the first 150 ns or so. Note that the electric field derivative waveform exhibits an initial negative field change due to the downward propagating leader, clearly evident in Figure 2b, prior to the positive derivative pulse from the upward propagating return stroke, as discussed by *Uman et al.* [2000]. The portion of the overall dE/dt waveform produced by the return stroke is of primary interest here. After about 150 ns, about 50 ns after the return stroke derivative peak, the electric field derivative decays more slowly than the current and magnetic field derivative waveforms, the latter two being very similar for their total duration, as evident in Figures 3 and 4.

4. Theory

[7] To examine the relationship between the field and current derivatives, we model the return stroke process using the transmission-line model [*Uman and McLain*, 1969], the simplest available and most used return stroke model, in which the return stroke channel current I is assumed to propagate in the upward direction along a straight arbitrarily oriented channel from ground level at constant speed v without waveform distortion or attenuation above a perfectly conducting Earth and is of the form

$$I(\ell', t) = I(0, t - \ell'/v), \tag{1}$$

where ℓ' is the coordinate along the return stroke channel whose origin is at ground level. For strokes S9934-6 and S9934-7 we model the channel as leaning at an angle $\theta = 20°$ from the vertical at a defined azimuthal angle $\varphi = 0$ (easterly direction), although, as noted earlier, the bottom 5 m or so of the channel was leaning toward the west. The electric field derivative antenna at 15 m is located at $\varphi = 120°$ and the electric field derivative antenna at 15 m at $\varphi = 135°$. The vertical electric field intensity (E) and the azimuthal magnetic flux density (B) at ground level a distance D from the bottom of a vertical ($\theta = 0$) channel are [*Uman et al.*, 1975; *Master et al.*, 1981]

$$E(D,t) = \frac{1}{2\pi\varepsilon_0}\int_0^{H(t)} \left(\frac{(2-3\sin^2\alpha)}{R^3}\int_{t_b(\ell')}^{t} I(\tau - \ell'/v - R/c)d\tau + \frac{(2-3\sin^2\alpha)}{cR^2} I(t-\ell'/v-R/c) - \frac{\sin^2\alpha}{c^2 R} \cdot \frac{\partial I(t-\ell'/v-R/c)}{\partial t} \right) d\ell', \tag{2}$$

$$B(D,t) = \frac{\mu_0}{2\pi}\sin\alpha \int_0^{H(t)} \left(\frac{1}{R^2} I(t-\ell'/v-R/c) + \frac{1}{cR}\frac{\partial I(t-\ell'/v-R/c)}{\partial t} \right) d\ell', \tag{3}$$

where ε_0 is the permittivity and μ_0 the permeability of free space, c is the speed of light, the lower integral limit $t_b(\ell')$ is the time at which the current is "seen" by the observer to begin at the channel section at length ℓ', while the upper integral limit $H(t)$ is the "radiating" length of the channel [see, e.g., *Thottappillil et al.*, 1997], R is the distance between the current element $d\ell'$ and the observation point, and α is the angle between the channel direction and a vector along the distance R from $d\ell'$ to the observation point on ground. The electric field is composed of, from left to right in equation (2), three components defined as the electrostatic field, the induction field, and the radiation field. The magnetic field is composed of, from left to right in equation (3), two components defined as the induction field and the radiation field [*Uman et al.*, 1975].

[8] For the case of the leaning channel the expressions equivalent to equations (2) and (3) are straightforward to derive and are found in equations (4) and (5):

$$E(D,t) = -\frac{1}{2\pi\varepsilon_0}\cos\theta \int_0^{L(t)} \left(\frac{R^2 + 3\,\ell'\,R\sin\alpha\sin\theta\cos\varphi - 3\ell'^2}{R^5} \cdot \int_{t_b(\ell')}^{t} I(\tau - \ell'/v - R/c)d\tau + \frac{R^2 + 3\,\ell'\,R\sin\alpha\sin\theta\cos\varphi - 3\ell'^2}{c\,R^4} \cdot I(t-\ell'/v-R/c) + \frac{R^2 + \ell' R\sin\alpha\sin\theta\cos\varphi - \ell'^2}{c^2 R^3} \cdot \frac{\partial I(t-\ell'/v-R/c)}{\partial t} \right) d\ell', \tag{4}$$

$$B(D,t) = -\frac{\mu_0}{2\pi}\cos\theta\sin\alpha \int_0^{L(t)} \left(\frac{1}{R^2} I(t-\ell'/v-R/c) + \frac{1}{c\,R} \cdot \frac{\partial I(t-\ell'/v-R/c)}{\partial t} \right) d\ell', \tag{5}$$

where $L(t)$ is the radiating length of the channel, θ is the angle between the z axis and the channel in the direction $\overline{\ell}'$, and φ is the angle between the horizontal component of the channel and a vector pointing from the bottom of the slanted

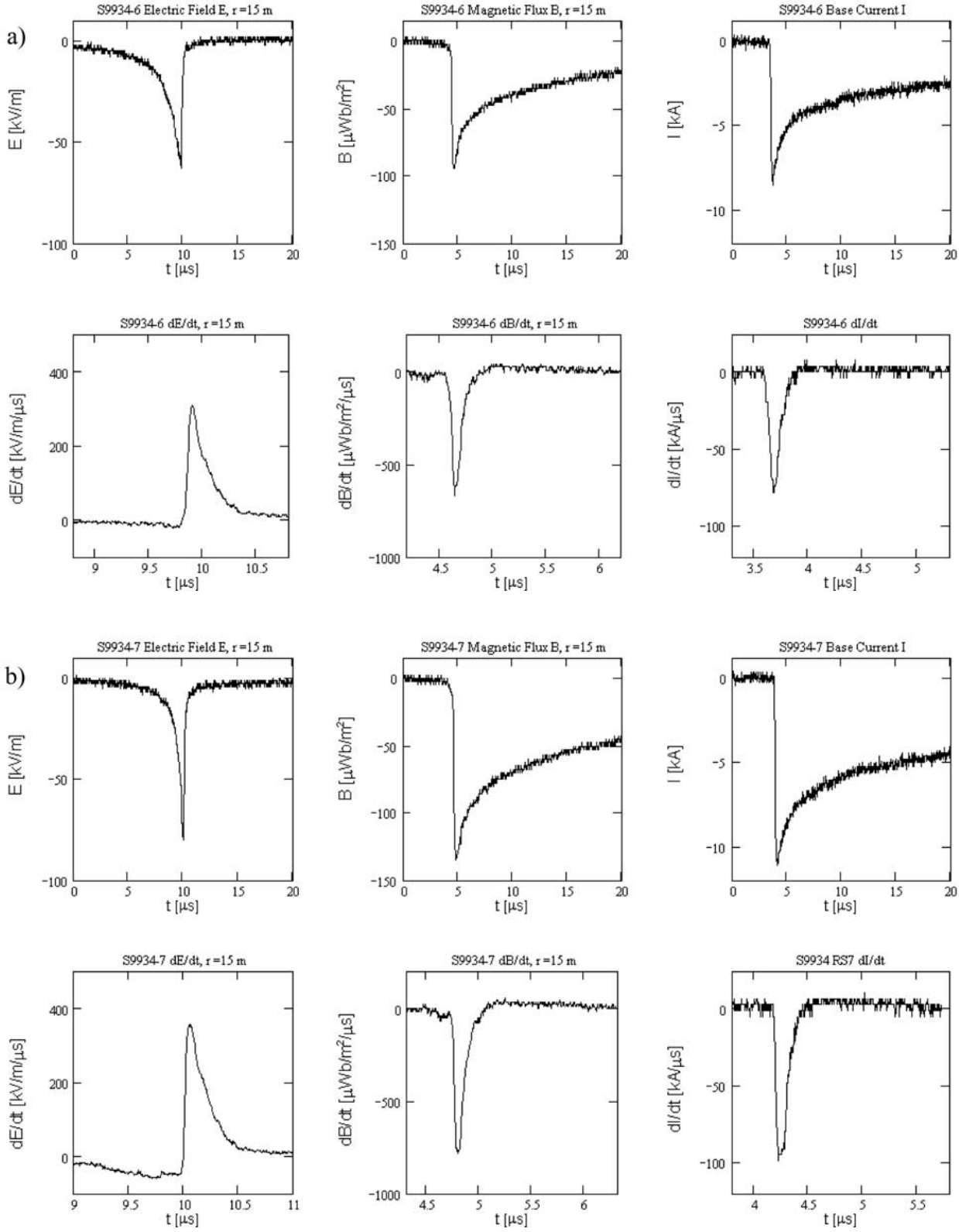

Figure 2. (a) For stroke S9934-6, a complete set of measurements (*I*, *dI/dt*, *E*, *dE/dt*, *B*, *dB/dt*), the latter four at 15 m. (b) For stroke S9934-7, a complete set of measurements (*I*, *dI/dt*, *E*, *dE/dt*, *B*, *dB/dt*), the latter four at 15 m.

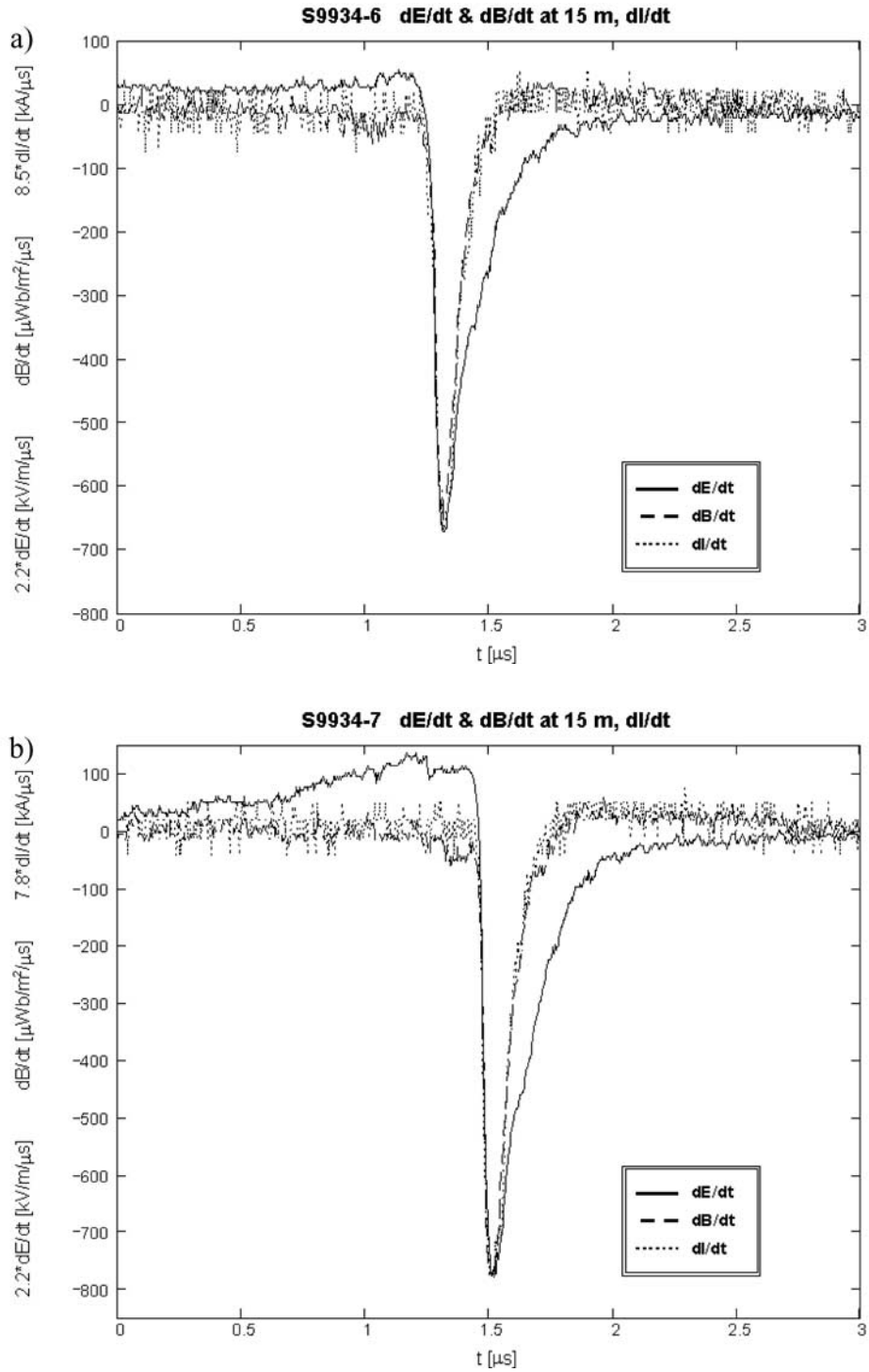

Figure 3. (a) Measured current derivative, magnetic flux density derivative, and negative of the electric field intensity derivative for S9934-6 on a 3-μs timescale. (b) Measured current derivative, magnetic flux density derivative, and negative of the electric field derivative for S9934-7 on a 3-μs timescale.

channel to the observation point. The observed current derivative at ground is the measured quantity that is used as one input to the transmission line model. In order to reduce noise in the calculated field derivative, the calculation being done by differentiating equations (4) and (5), the measured current derivative was filtered with a third order, 20-MHz elliptic low-pass filter. Linear interpolation was used between the filtered data points. The second input to the model is the return stroke speed, which is not known. We perform the model calculation for three assumed values of speed, 1×10^8 m s^{-1}, 2×10^8 m s^{-1}, and 3×10^8 m s^{-1} (the speed of light). Comparison of the model-predicted waveforms for the three speeds with the experimental data provides some insight into the

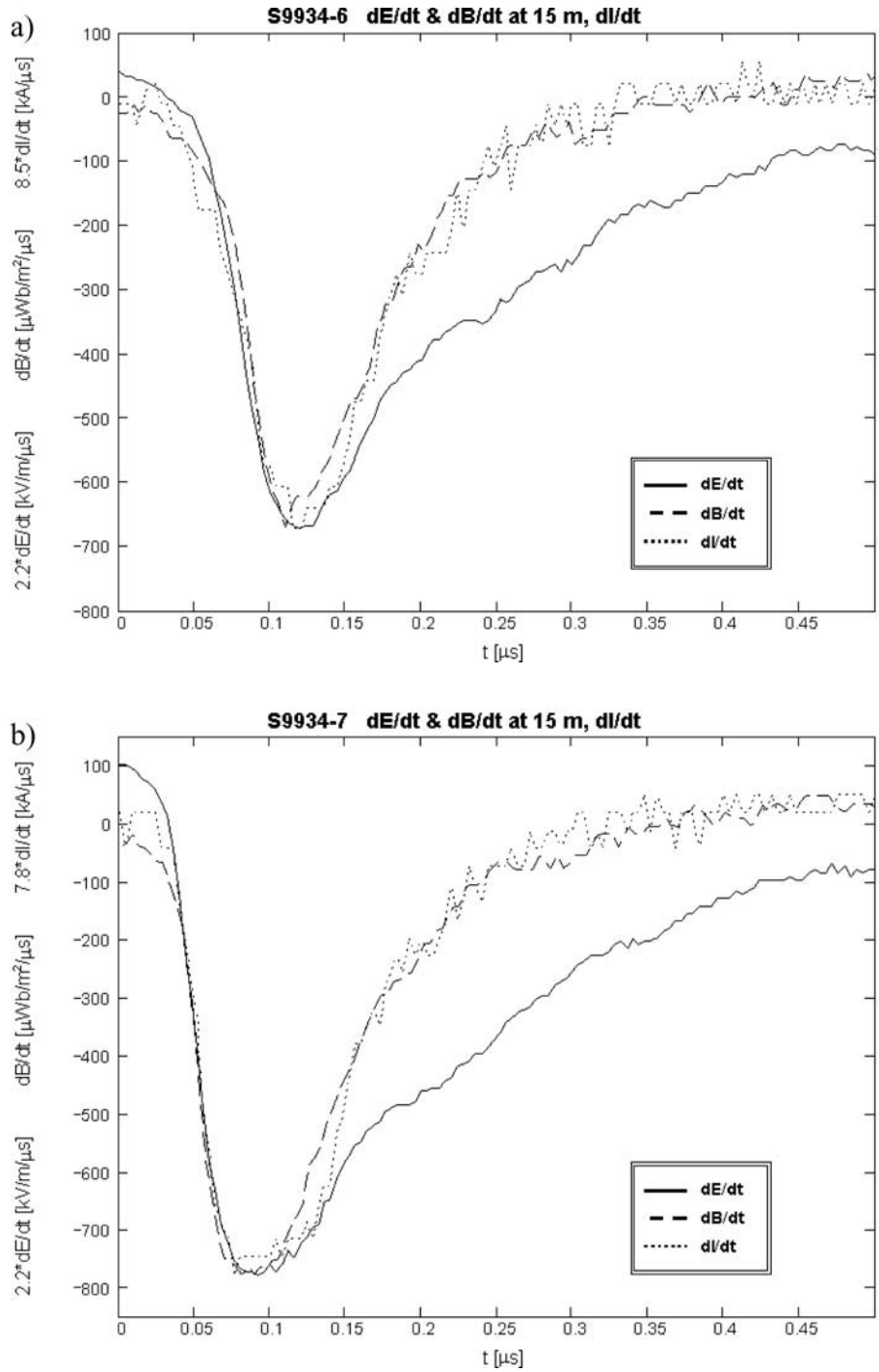

Figure 4. (a) Measured current derivative, magnetic flux density derivative, and negative of the electric field intensity derivative for S9934-6 on a 0.5-μs timescale. (b) Measured current derivative, magnetic flux density derivative, and negative of the electric field derivative for S9934-7 on a 0.5-μs timescale.

actual speed, assuming that the model provides a reasonable representation of the physics of the situation. In Figures 5a and 5b we show the calculated (for three speeds) and measured magnetic field derivatives and electric field derivatives, respectively, for stroke 6 in flash S9934. A similar data presentation for S9934-7 is found in Figures 6a and 6b. The magnetic field derivative comparisons in Figures 5a and 6a indicate a reasonable model fit to the data in waveshape and amplitude for a return stroke speed near 2×10^8 m s^{-1}. The electric field derivative waveshape matches are reasonable for a similar or higher speed, but the amplitude of the calculated derivatives is less than the observed values (Figures 5b and 6b). As noted in section 2, the antenna calibrations are thought to be accurate to about 20%. Clearly, a model return stroke speed of 1×10^8 m s^{-1} does not provide a

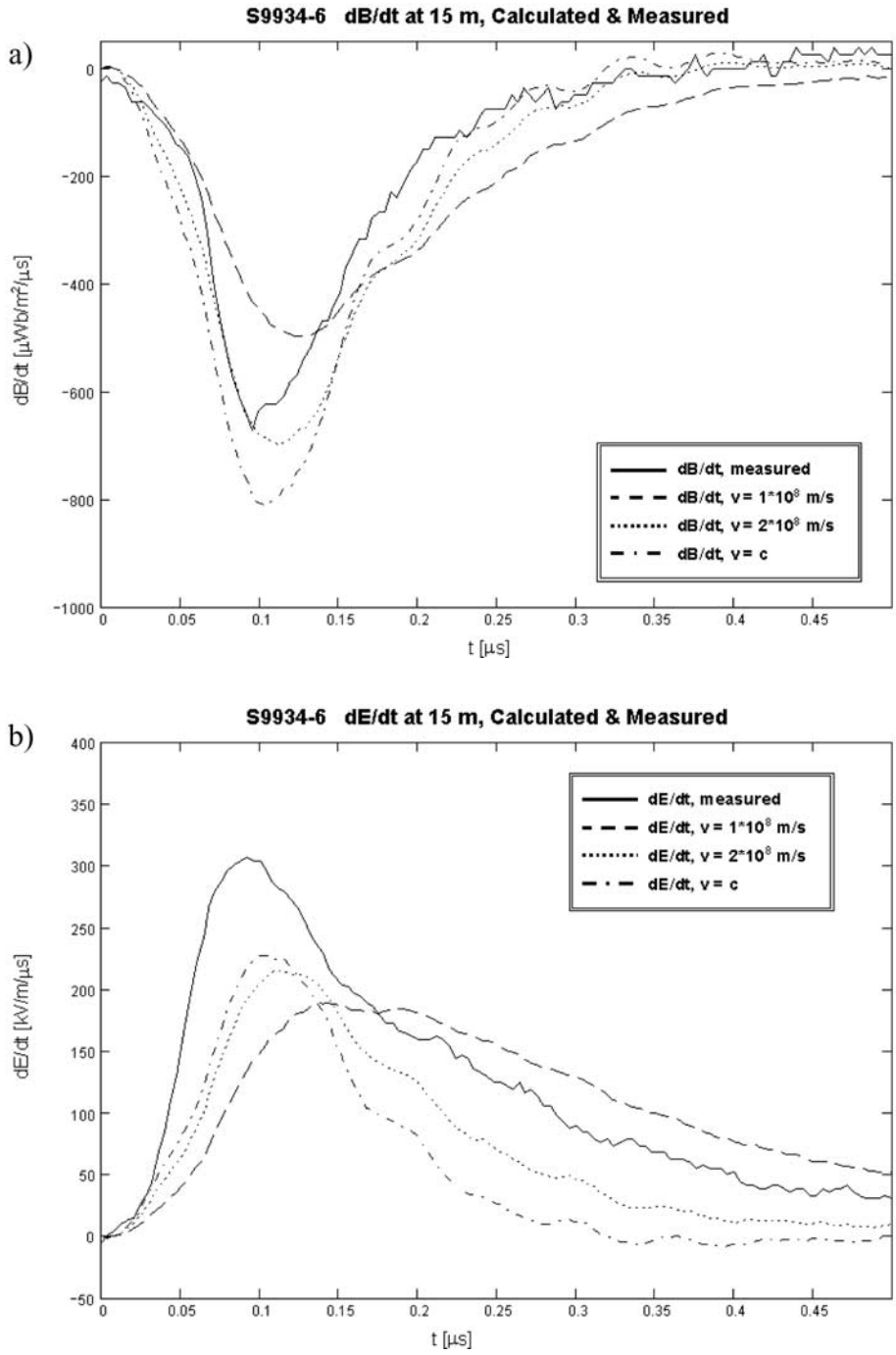

Figure 5. (a) Comparison of measured and model-predicted magnetic flux density derivatives for three return stroke speeds for S9934-6. (b) Comparison of measured and model-predicted electric field intensity derivatives for three return stroke speeds for S9934-6.

reasonable fit to any of the experimental waveforms, while a model speed between 2×10^8 m s^{-1} and the speed of light provides the best overall fit to the measured data.

[9] One interesting aspect in the modeling is worth noting. The calculated waveshape of the magnetic field derivative does not approximate the waveshape of the current derivative for return stroke speeds of 1×10^8 m s^{-1} or 2×10^8 m s^{-1}, as is the case for the experimental data, but it does for the speed of light, at which speed the calculated electric and magnetic field derivative waveshapes and the input current derivative waveshape all become identical, as has been shown analytically from theory for the transmission-line model with a vertical channel by *Thottappillil et al.* [2001]. At the speed of light the peak of the calculated electric field derivative at 15 m for S9934-6 and S9934-7 is 0.74 times and 0.81 times the measured peak field derivative, respectively, and the peak of the calculated magnetic field derivative for S9934-6 and

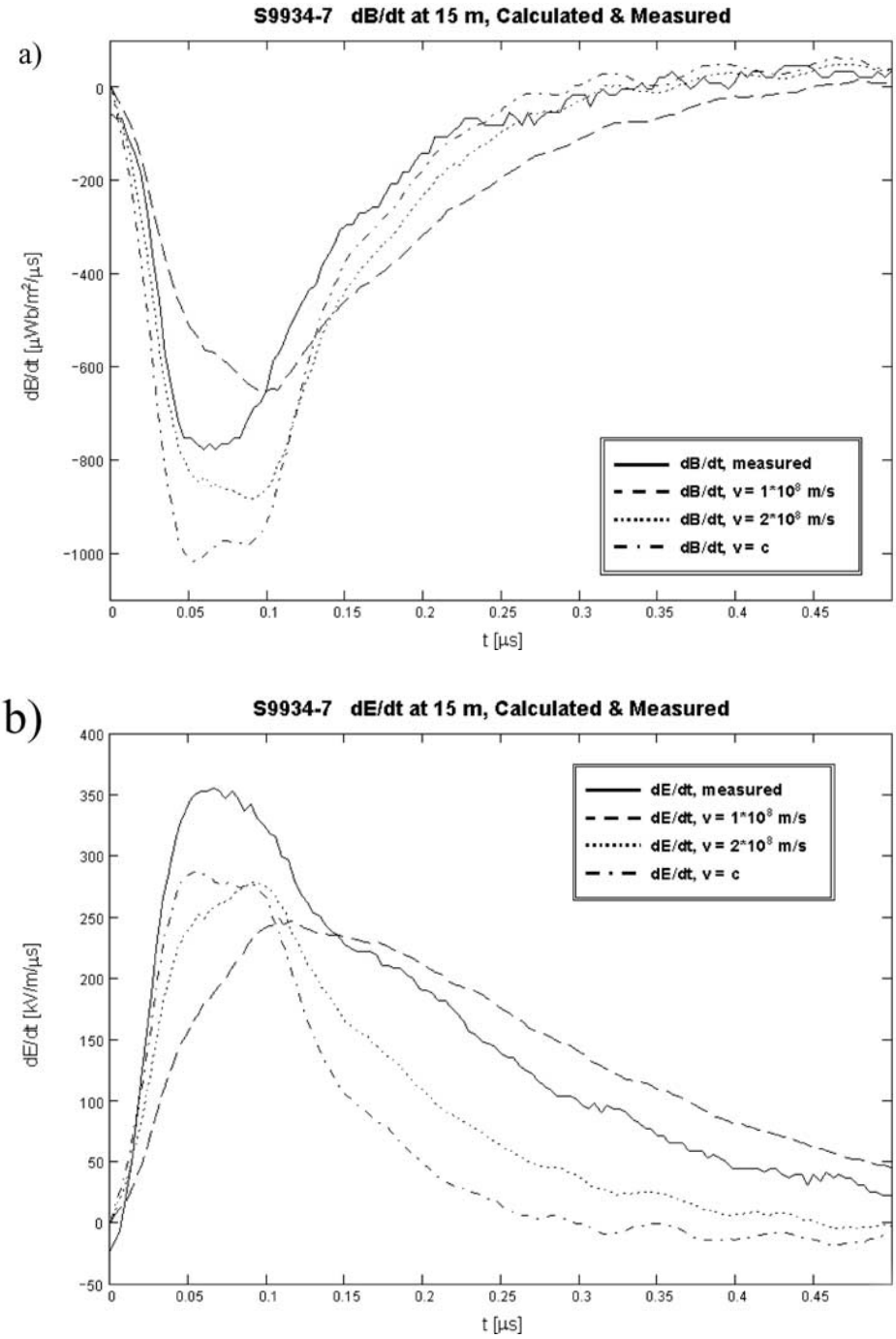

Figure 6. (a) Comparison of measured and model-predicted magnetic flux density derivatives for three return stroke speeds for S9934-7. (b) Comparison of measured and model-predicted electric field intensity derivatives for three return stroke speeds for S9934-7.

S9934-7 is 1.21 times and 1.31 times the measured field peak, respectively.

5. Discussion

[10] *Baker et al.* [1987] have measured the electric field derivative and the magnetic field derivative for one triggered lightning stroke that struck a 20-m conducting mast. Waveforms were recorded 60 m from the base of the mast. The waveforms, given in *Baker et al.*'s [1987] Figures 7 and 9, do not show a discernable rise to peak on the scale that they are presented, but the decay of each waveform after peak is similar to that of our waveforms. To model their measured fields, *Baker et al.* [1987] use the transmission line model for a vertical return stroke channel (our equations (1)–(3)) with the return stroke current being launched upward from the top of the 20-m strike object. They apparently ignore the effects of the downward propagating

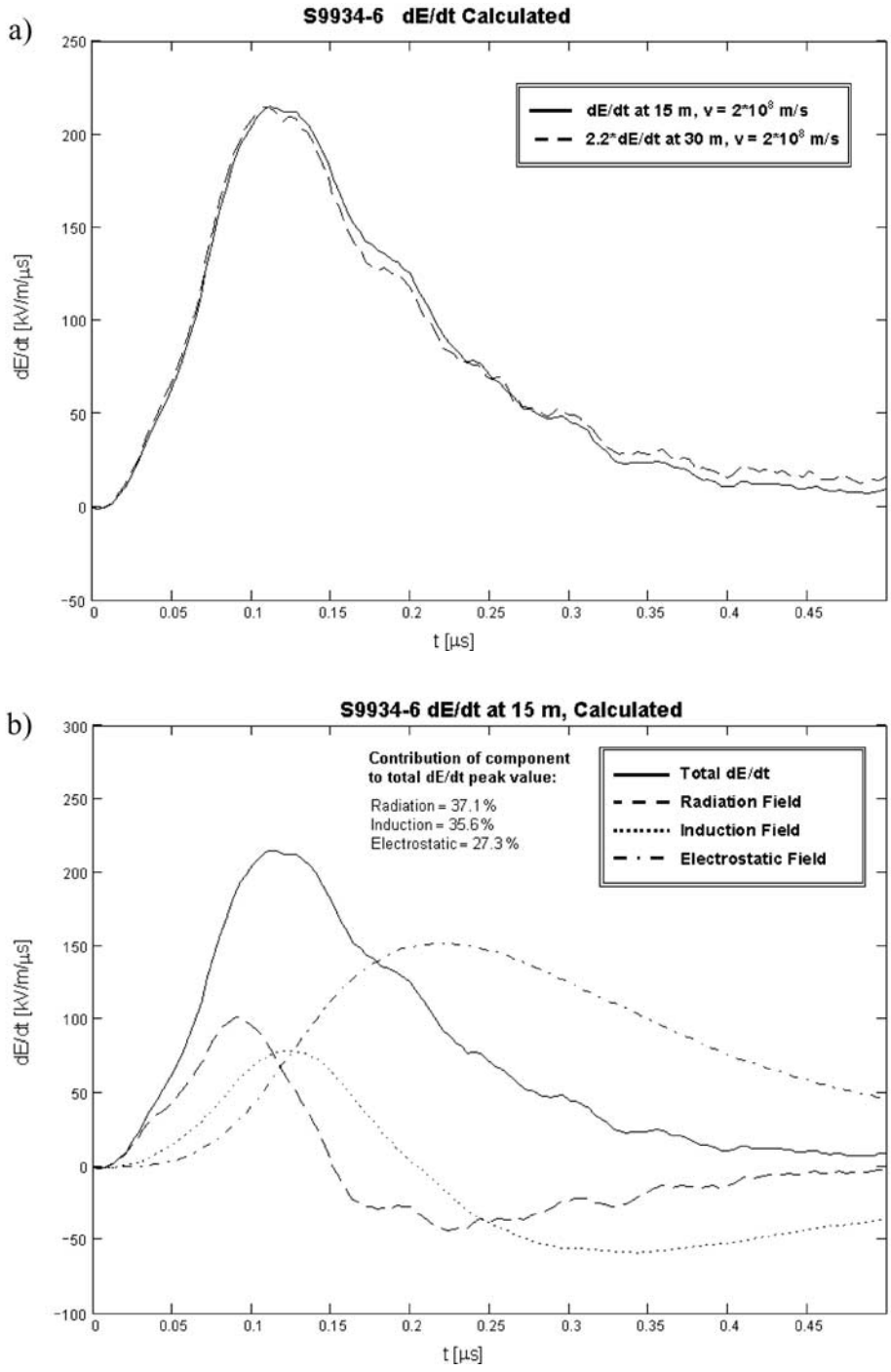

Figure 7. (a) Comparison of the calculated total electric field intensity derivatives at 15 m and at 30 m for S9934-6. (b) Calculated components of the electric field intensity derivative at 15 m for S9934-6 with $v = 2 \times 10^8$ m s^{-1}. (c) Calculated components of the electric field intensity derivative at 30 m for S9934-6 with $v = 2 \times 10^8$ m s^{-1}.

current in the strike object, although the fields from current in that 20-m object could well be significant or even dominant at 60 m [*Leteinturier et al.*, 1990] (see also last paragraph of this section). Additionally, they model the measured current with a double-exponential function, $I = 17$ $[\exp(-t/0.24 \times 10^{-6} - \exp(-t/25 \times 10^{-6})]$ kA. With such a function the peak current derivative, needed in the model, occurs at the initiation of the current waveform, $t = 0$, whereas our measured current derivatives exhibit peaks at 50 to 100 ns (Figures 4a and 4b). Thus there are significant questions about the validity of the modeling of *Baker et al.* [1987]. *Baker et al.* [1987] conclude from their modeling that the best match between their measured field derivatives and those calculated from the transmission line model, in the manner described above, is for a return stroke speed of 0.9 times the speed of light c, 2.7×10^8 m s^{-1}. It is not

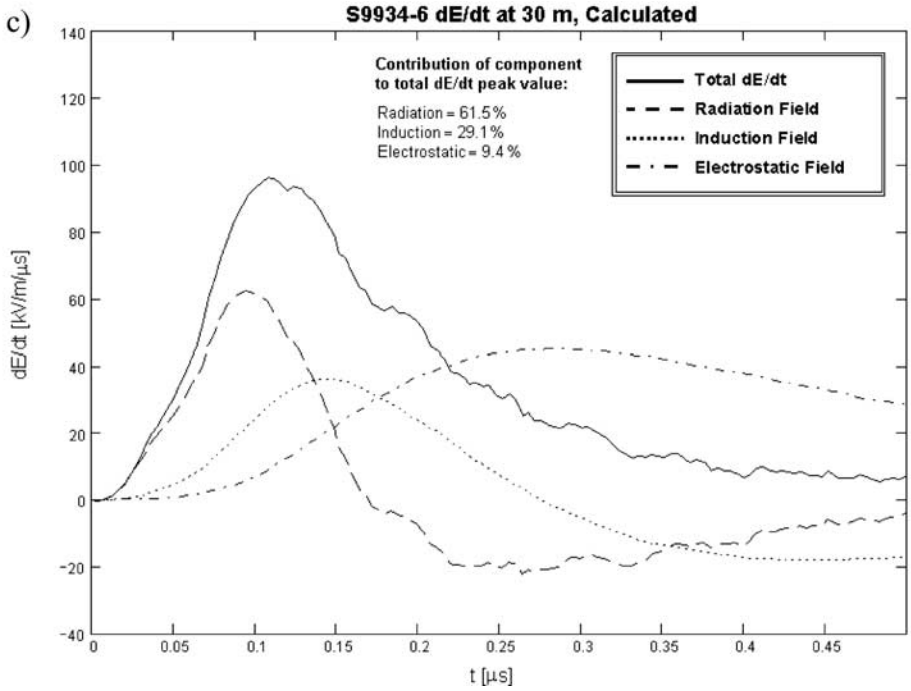

Figure 7. (continued)

possible to tell from *Baker et al.*'s [1987] Figures 7 and 9 how good the match between theory and measurement is at the peak field derivatives, but the theoretical waveform decays follow the measured decays. In the experiment described in the present paper, the strike rod was intentionally made relatively small, 2 m, in an effort to minimize its effects on the fields and to make possible a straightforward application of the transmission line model. Note that the downside of our use of a small strike rod is that in our experiments the triggered lightning often struck ground around the rod or struck the rocket-launching assembly rather than striking the 2-m rod.

[11] We consider now the issue of the relative amplitude of the components (electrostatic, induction, and radiation) in the close field derivative waveforms discussed by *Uman et al.* [2000], in consideration of the arguments that field derivative and current derivative waveform similarities and field derivative waveshape similarities at different distances imply a dominant radiation field. We did not record the electric field derivative at 30 m for flash S9934 because of an equipment malfunction. However, for many sets of electric field derivative waveforms that we did measure simultaneously in 1999 at both 15 and 30 m, the electric field derivative waveshapes were observed to be similar, as previously reported by *Uman et al.* [2000] to be the case at 10 and 30 m and as suggested by them to be potential evidence for a dominant radiation field component. The relative invariance of the waveform with distance is also predicted by the transmission line model, the total calculated electric field derivative at 15 m and at 30 m being compared in Figure 7a for S9934-6 with $v = 2 \times 10^8$ m s^{-1}. In fact, our transmission-line calculations show that the electric field derivative waveshapes at 15 m and at 30 m are very similar for return stroke speeds between about 1.5×10^8 m s^{-1} and the speed of light for either the slanted channel or a vertical channel. However, while the field derivatives are similar at the two distances, the mix of field components calculated using the transmission line model changes significantly from 15 to 30 m, as shown in Figures 7b and 7c for the case calculated in Figure 7a. The radiation component is less than half the peak electric field derivative at 15 m and somewhat over half at 30 m. It is of value to note that *Thottappillil and Rakov* [2001] have shown analytically that the traditional division of field components given in equations (2) and (3) or equations (4) and (5) is not unique and that the fields may be analytically divided in other ways while maintaining the same total fields. In any event, it is clear that although the measured electric field, magnetic field, and current derivative waveforms appear similar for the initial 150 ns, this observation is not due to a dominant radiation field, as previously suggested might be the case by *Leteinturier et al.* [1990] and by *Uman et al.* [2000]. Our calculations are consistent with the transmission line calculations of *Cooray* [1989] (for a vertical channel), who found that for a return stroke speed of 2×10^8 m s^{-1} the ratio of total peak electric field derivative to radiation field derivative at 50 m was between 1.3 and 1.5 depending on assumed current waveshape, and of *Leteinturier et al.* [1990], who, using a measured current derivative waveform, found that the ratio of total peak electric field derivative to the radiation field derivative was 1.2 for the same distance and speed.

[12] The expressions

$$\frac{dE(D,t)}{dt} = -\frac{v}{2\pi\varepsilon_0 c^2 D}\frac{dI(0,t-D/c)}{dt} \tag{6}$$

$$E = cB \tag{7}$$

can be derived from equations (2) and (3) for the case of a dominant radiation field and $\alpha \cong 90°$, that is, a radiation

field source near ground level [*Uman et al.*, 1975]. Equation (6) has been used by *Leteinturier et al.* [1990] and *Uman et al.* [2000] to determine return stroke speed from measured electric field derivative and current derivative peaks for triggered lightning strokes between 10 and 50 m assuming that the field derivatives were dominated by the radiation component. Those calculated speeds were, on average, near the speed of light, some being greater. From equation (6) for S9934-6 and S9934-7 we find at 15 m speeds of 2.9×10^8 m s^{-1} and 2.7×10^8 m s^{-1}, respectively, and using the measured magnetic field derivative peaks and equations (6) and (7), 1.9×10^8 m s^{-1} and 1.8×10^8 m s^{-1}, respectively. Clearly, the reason that the return stroke speed derived assuming a dominant electric field derivative radiation component exceeds the speed found by matching measured and calculated electric and magnetic field derivatives using equations (4) and (5) is that the radiation field component is not dominant, a conclusion that *Leteinturier et al.* [1990] stated ''seems fairly clear'' in referring to their 50-m data. In fact, at 15 and 30 m, there is not a dominant field derivative component. *Willett et al.* [1989] used equation (6) and triggered lightning electric field derivative measurements at about 5 km, a distance at which theory indicates that the electric field derivative is indeed dominated by the radiation component, to derive return stroke speed values near 2×10^8 m s^{-1}, a result similar to the speeds inferred for the two strokes at 15 m in the present study using equations (4) and (5).

[13] In modeling the two return strokes S9934-6 and S9934-7 using the transmission-line model, we have not taken account of the detailed geometry of the channel and of any effects that might be associated with the 2-m strike rod and with potential upward going connecting leaders initiated at the top to the rod prior to return stroke formation. *Wang et al.* [1999] found upward connecting leader lengths of 7–11 m and 4–7 m for two strokes with peak currents of 21 kA and 12 kA, respectively, the peak currents for the two strokes in the present experiment being 11 and 8.5 kA. If the upward connecting leader length and the return stroke current are roughly proportional, as might be expected on physical grounds and as appears to be the case from the data of *Wang et al.* [1999], the upward connecting leader lengths for S9934-6 and S9934-7 might be expected to be in the range 3 to 6 m, perhaps accounting for the fact that the lowest 5 m or so of the S9934 channel was oriented at a different angle to the vertical than was the channel above it. The return stroke can be viewed as starting at the top of the upward connecting leader and propagating both upward and downward, with some fraction of the downward wave reflecting upward from the strike object and also from the ground. For example, for a 4-m upward connecting leader and a return stroke speed of 2×10^8 m s^{-1}, reflections on a 20-ns timescale might be expected. Propagation speeds in the 2-m strike rod are expected to be the speed of light, so reflections associated with the rod are on a shorter timescale. Perhaps taking the effects associated with channel geometry, the upward leader, and the strike rod into account would improve the agreement between measurement and modeling in the context of the transmission line model. On the other hand, perhaps the transmission line model is not the best model to describe return stroke behavior. *Rakov and Uman* [1998] have discussed a number of models that can be applied to the return stroke.

[14] **Acknowledgments.** This research was supported in part by FAA grant 99-G-043 and NSF grants ATM-9726100 and ATM-0003994.

References

Baker, L., R. L. Gardner, A. H. Paxton, C. E. Baum, and W. Rison, Simultaneous measurement of current, electromagnetic fields, and optical emission from a lightning stroke, *Electromagnetics*, *7*, 441–450, 1987.

Cooray, V., Derivation of return stroke parameters from electric and magnetic field derivatives, *Geophys. Res. Lett.*, *16*, 61–64, 1989.

Crawford, D. E., V. A. Rakov, M. A. Uman, G. H. Schnetzer, K. J. Rambo, M. V. Stapleton, and R. J. Fischer, The close lightning electromagnetic environment: Dart-leader electric field change versus distance, *J. Geophys. Res.*, *106*, 14,909–14,917, 2001.

Leteinturier, C., C. Weidman, and J. Hamelin, Current and electric field derivatives in triggered lightning return strokes, *J. Geophys. Res.*, *95*, 811–828, 1990.

Master, M. J., M. A. Uman, Y. T. Lin, and R. B. Standler, Calculations of lightning return stroke electric and magnifields above ground, *J. Geophys. Res.*, *86*, 12,127–12,132, 1981.

Rakov, V. A., and M. A. Uman, Review and evaluation of lightning return stroke models including some aspects of their application, *IEEE Trans. Electromagn. Compat.*, *40*, 403–426, 1998.

Rakov, V. A., et al., New insights into lightning processes gained from triggered-lightning experiments in Florida and Alabama, *J. Geophys. Res.*, *103*, 14,117–14,130, 1998.

Thottappillil, R., and V. A. Rakov, On different approaches to calculating lightning electric fields, *J. Geophys. Res.*, *106*, 14,191–14,206, 2001.

Thottappillil, R., V. A. Rakov, and M. A. Uman, Distribution of charge along the lightning channel: Relation to remote electric and magnetic fields and to return-stroke models, *J. Geophys. Res.*, *102*, 6987–7006, 1997.

Thottappillil, R., J. Schoene, and M. A. Uman, Return stroke transmission line model for stroke speed near and equal that of light, *Geophys. Res. Lett.*, *28*, 3593–3596, 2001.

Uman, M. A., and D. K. McLain, The magnetic field of the lightning return stroke, *J. Geophys. Res.*, *74*, 6899–6910, 1969.

Uman, M. A., D. K. McLain, and E. P. Krider, The electromagnetic radiation from a finite antenna, *Am. J. Phys.*, *43*, 33–38, 1975.

Uman, M. A., V. A. Rakov, G. H. Schnetzer, K. J. Rambo, D. E. Crawford, and R. J. Fisher, Time derivative of the electric field 10, 14, and 30 m from triggered lightning strokes, *J. Geophys. Res.*, *105*, 15,577–15,595, 2000.

Wang, D., V. A. Rakov, M. A. Uman, N. Takagi, T. Watanabe, E. Crawford, K. J. Rambo, G. H. Schnetzer, R. J. Fisher, and Z. I. Kawasaki, Attachment process in rocket-triggered lightning strokes, *J. Geophys. Res.*, *104*, 2143–2150, 1999.

Willett, J. C., J. C. Bailey, V. P. Idone, A. Eybert-Berard, and L. Barret, Submicrosecond intercomparison of radiation fields and currents in triggered lightning return strokes based on the transmission line model, *J. Geophys. Res.*, *94*, 13,275–13,286, 1989.

V. A. Rakov, K. J. Rambo, G. H. Schnetzer, J. Schoene, and M. A. Uman, Department of Electrical and Computer Engineering, University of Florida, Gainesville, Florida 32611, USA. (rakov@ece.ufl.edu; rambo@tec.ufl.edu; gschnetzer@zianet.com; jenss@ufl.edu; uman@ece.ufl.edu)